Riemann Problems for the Two-Dimensional Unsteady Transonic Small Disturbance Equation

Sunčica Čanić*
Department of Mathematics
Iowa State University
Ames, Iowa 50011

Barbara Lee Keyfitz†
Department of Mathematics
University of Houston
Houston, Texas 77204-3476

Abstract. We study a two-parameter family of Riemann problems for the UTSD equation, also called the two-dimensional Burgers equation, which is used to model the transition from regular to Mach reflection for weak shock waves. The related initial-value problem consists of oblique shock data in the upper half plane, with two parameters a and b corresponding to the slopes of the initial shock waves. The study of quasi-steady solutions leads to a problem that changes type when written in self-similar coordinates. The problem is hyperbolic in the region where the flow is supersonic, and elliptic where the flow is subsonic.

In this paper we give a complete description of the flow in the hyperbolic region by resolving the hyperbolic wave interactions in the form of quasi-one-dimensional Riemann problems. In the region of physical space where the flow is subsonic, we pose the related free-boundary problems and discuss the behavior of the subsonic solution using results from our previous work. Based on this approach we establish the existence of regions of different qualitative behavior in parameter (a, b) space. Our results reveal that the UTSD equation seems to be particularly suitable for the study of the so called von Neumann paradox in which linearly degenerate waves can be ignored. We establish the region in the parameter space where a prototype of von Neumann reflection takes place. In other regions of parameter space we find prototypes for Mach reflection, regular reflection, and transitional Mach reflection. The lack of linearly degenerate waves in this model is resolved by the presence of a small rarefaction wave emerging from the triple point.

Key words. Two-dimensional Riemann problems, unsteady transonic

*Supported by the Department of Energy, grant DE-FG02-94ER25220, and in part by the NSF under grant DMS-9403598. Support by the Energy Laboratory and the Department of Mathematics at the University of Houston is also acknowledged.

†Research supported by the Texas Advanced Research Program under Grant 00365-2102-ARP and the Department of Energy, grant DE-FG03-94ER25222.

small-disturbance equation.

AMS subject classification. Primary: 35L65, 35L37; Secondary: 35M10

Contents

List of Figures

1. INTRODUCTION

This paper reports on a study of the unsteady transonic small disturbance equation

$$\begin{aligned} u_t + uu_x + v_y &= 0\,, \\ -v_x + u_y &= 0\,. \end{aligned} \tag{1.1}$$

An initial summary was given in [9]. This equation models the transition between Mach and regular reflection for weak shocks and small wedge angles. Based on the work of Brio and Hunter, [3], we consider Riemann data consisting of three states in the upper half plane, separated by shocks. The boundary data on the x-axis are $u_y = 0 = v$. We consider the *oblique shock interaction problem* with states

$$\begin{cases} U_0 &= (0,0) \\ U_1 &= (1,-a) \\ U_2 &= (1+a/b,0) \end{cases} \tag{1.2}$$

(see Figure 1.1) and initial discontinuities on the lines $x = ay$ and $x = -by$. This results in discontinuities which propagate as shocks.

In this paper we show that the two-parameter problem displays qualitative features similar to those seen in a number of studies of shock interaction problems [2, 11, 12, 13, 14, 15, 16].

Most of this paper is devoted to solving and reducing the self-similar problem to the point where the subsonic problem can be identified and studied. In other work, we have begun an analysis of the subsonic problem, [4, 8, 6]. Based on our experience with this problem, we offer some conjectures on what the subsonic analysis may reveal. Numerical results in [10] confirm those conjectures. In Section 2 we propose a bifurcation diagram

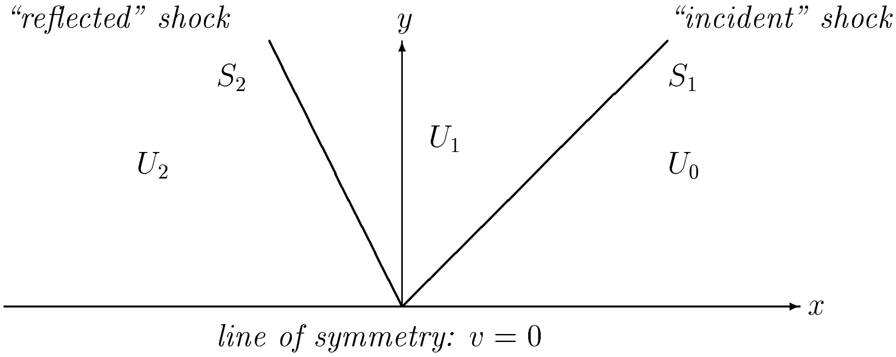

Figure 1.1: Riemann Data for a Shock Reflection Problem

in (a, b)-parameter space based on preliminary wave analysis. In Sections 3 and 4, we outline the free-boundary problems that arise in the interaction between hyperbolic waves and the subsonic (elliptic) region. We summarize our conclusions in Section 5 and give a revised bifurcation diagram based on hyperbolic wave interactions and subsonic flow behavior.

Our approach here, based strongly on similarity solutions and the corresponding dimension reduction that results, does not say anything about multi-dimensional flows which are not self-similar (quasi-steady). However, Riemann problems in one-dimensional gas dynamics have played a very important role which may extend to two-dimensional problems. In addition, self-similar solutions are used to model prototype shock reflection problems, as described above.

Self-similar analysis suggests that there may be more than one solution for certain configurations of data. We prove in Theorem 3.1 that this is indeed the case. This is in the nature of bifurcation problems. Because of the construction we are using, we believe that all the solutions we find and conjecture are stable to small perturbations of the Riemann data, to perturbation by smoothing of the data, or to viscous perturbation of the equations.

In self-similar coordinates, $\xi = x/t$, $\eta = y/t$, equation (1.1) becomes

$$\begin{aligned} (u-\xi)u_\xi - \eta u_\eta + v_\eta &= 0\,, \\ -v_\xi + u_\eta &= 0\,. \end{aligned} \tag{1.3}$$

This can be written as a quasilinear system

$$\begin{aligned} A(U,\Xi)U_\xi + B(U,\Xi)U_\eta &\equiv \left[\begin{pmatrix} u-\xi & 0 \\ 0 & -1 \end{pmatrix}\partial_\xi + \begin{pmatrix} -\eta & 1 \\ 1 & 0 \end{pmatrix}\partial_\eta\right]\begin{pmatrix} u \\ v \end{pmatrix} \\ &= 0 \end{aligned} \tag{1.4}$$

or in conservation form

$$\begin{aligned} \partial_\xi F(U,\Xi) + \partial_\eta G(U,\Xi) &\equiv \partial_\xi \begin{pmatrix} u^2/2 - \xi u \\ -v \end{pmatrix} + \partial_\eta \begin{pmatrix} v - \eta u \\ u \end{pmatrix} \\ &= S \equiv \begin{pmatrix} -2u \\ 0 \end{pmatrix} \end{aligned} \tag{1.5}$$

with $U = (u,v)$ and $\Xi = (\xi,\eta)$.

Now, from (1.4) it can easily be seen that the system changes type; it is hyperbolic outside and elliptic inside the parabola

$$P_u: \qquad \xi + \frac{\eta^2}{4} = u.$$

The characteristics in the hyperbolic region are straight lines (when the equation is linearized about a constant state) tangent to P_u. See Figure 1.2.

In addition, shocks between constant states, from (1.5) (see Section 3.1), have the form

$$\xi = \kappa\eta + \omega$$

where

$$\kappa \equiv -\frac{[v]}{[u]} = -\frac{v_L - v_R}{u_L - u_R}; \qquad \omega \equiv \kappa^2 + \frac{u_L + u_R}{2}.$$

In the next section we identify the geometry of the elementary configurations corresponding to the states in this problem.

2. The Geometry of Primary Intersections

The following geometric objects play a role in the analysis.

Shocks: S_1 (between U_0 and U_1): $\xi = a\eta + (1/2 + a^2) \equiv \kappa_1\eta + \omega_1$
S_2 (between U_1 and U_2): $\xi = -b\eta + (1 + a/2b + b^2) \equiv \kappa_2\eta + \omega_2$

Parabolas: P_0: $\xi = -\eta^2/4$
P_1: $\xi = -\eta^2/4 + 1$
P_2: $\xi = -\eta^2/4 + 1 + a/b$

(Each P_i is the change of type locus for the state U_i.)

Axis of Symmetry W (wall): $\eta = 0$

These six objects define the *primary curves* of the problem: they are intrinsically defined in terms of the quasi-one-dimensional data for the reduced problem (1.3). We consider the data for this problem to be "Cauchy

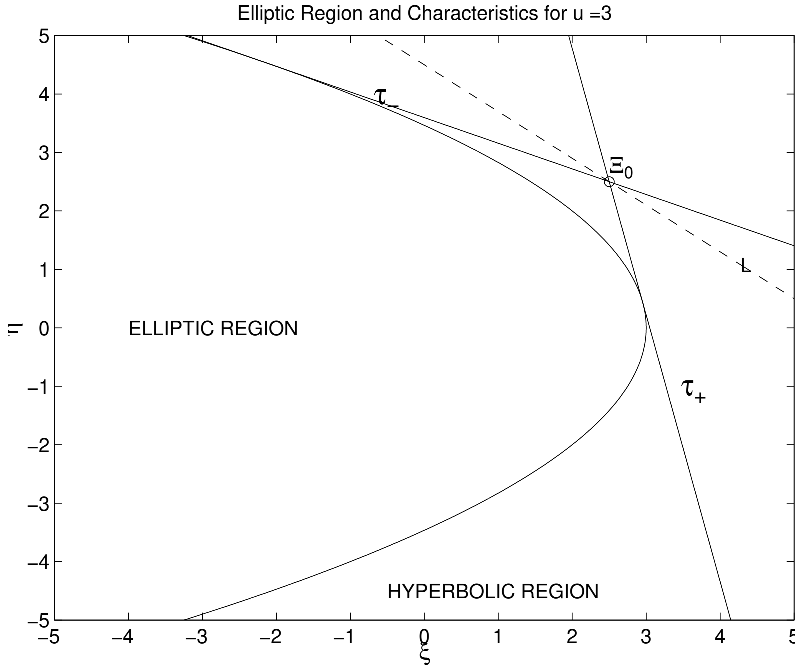

Figure 1.2: The Hyperbolic and Elliptic Regions in (ξ, η)

data given at infinity", corresponding to Riemann data for the original two-dimensional problem given at $t = 0$, since $|\Xi| \to \infty$ as t decreases to zero. In fact, the negative x-axis is not appropriate for giving data, because (1.1) is not hyperbolic in time: we should consider data given on a parabolic arc

$$\xi + \eta^2/4 = C \tag{2.1}$$

for sufficiently large C. As long as we are considering simple data of the form (1.2) the exact nature of this curve is not important.

Using the linearized equation, we can define the *domain of influence* of a point to be the union of the forward wave cone through the point and the parabola. For a point (ξ, η) one can also define the *domain of dependence* by following the characteristics of (1.4) back to (2.1). For arbitrary piecewise constant data at infinity (or on (2.1)) we can define the *quasi-one-dimensional domain of determinacy*: assuming all the quasi-one-dimensional Riemann problems can be solved locally (as in the next section), there is a region of (ξ, η) space outside of (or "before") any intersections of the primary curves take place. To help in categorizing the different cases which may arise, we define

Definition 2.1 *The* primary intersections *are all the points* Ξ *at which the primary curves could intersect and generate new waves. These points, for*

Intersection	Name	Point
$S_1 \cap S_2$	Ξ_I	$(1/2 + a/2b + ab, 1/2b + b - a)$
$S_2 \cap P_2$	Ξ_0	$(1 + a/2b - b^2 - \sqrt{2ab}, 2b + \sqrt{2a/b})$
	Ξ_*	$(1 + a/2b - b^2 + \sqrt{2ab}, 2b - \sqrt{2a/b})$
$S_1 \cap P_1$	Ξ_1	$(-a^2 + a\sqrt{2} + 1/2, -2a + \sqrt{2})$
$S_1 \cap W$	Ξ_A	$(\omega_1, 0) = (1/2 + a^2, 0)$
$S_2 \cap W$	Ξ_B	$(\omega_2, 0) = (1 + a/2b + b^2, 0)$
$S_1 \cap P_2$		$(-a^2 + 1/2 + \sqrt{2a + 4a^2/b}, -2a + \sqrt{2 + 4a/b})$

Table 2.1: The Primary Intersections

our problem, are $S_1 \cap S_2$, $S_i \cap W$ and $S_i \cap P_i$ for $i = 1$ and 2.

For convenience, we label all points, even though some of them are in the lower half-plane for some parameter values. The list is in Table 2.1; a sketch in Figure 2.1 identifies the points.
Remark: It is clear that intersections of one shock with another, or of a shock with the wall, generate new waves. But the point where a shock intersects the parabola corresponding to one state of the shock may mark a transition from uniform to nonuniform flow, as we shall explore.

Not all the primary intersections actually occur in the solution of the Riemann problem; some never occur, and some occur or not depending on the values of a and b. A primary intersection will occur if it is not in the domain of influence of any other intersection or of nonconstant data on (2.1). Because the characteristics in the hyperbolic region are easily computed (Figure 1.2), it is straightforward to compute the forward domain of influence of any point. The elliptic regions are conveniently nested, based on the magnitude of the data. However, there is no maximum principle: data at infinity may generate states of larger magnitude, and hence an *a priori* computation of the backwards domain of dependence of any point is not possible.

Definition 2.2 *An* admissible intersection *is one that is completely determined by the data at infinity.*

We can determine the admissible intersections for different ranges of a and b. The following elementary propositions were proved in [9].

Proposition 2.1 *If Ξ_I is upstream from Ξ_0 then it is admissible.*

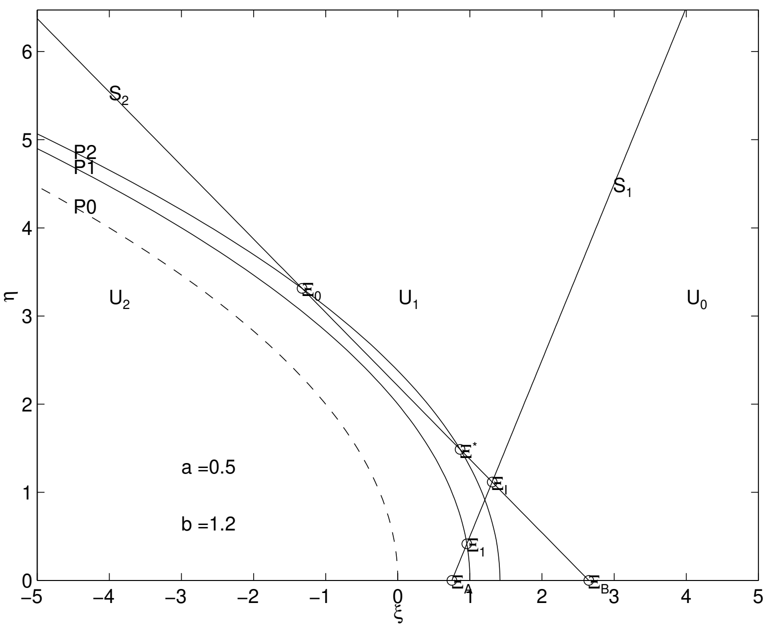

Figure 2.1: Sketch of Primary Intersection Points

Now, this occurs if $\eta_I \geq \eta_0$. This is the case if $b < 1/\sqrt{2}$ and

$$a \leq \frac{3}{2b} - b - \sqrt{2}\sqrt{\frac{1}{b^2} - 1} \equiv I(b).$$

Note that Ξ_I is outside P_2 when

$$a^2 + (2b - 3/b)a + 1/(4b^2) + b^2 - 1 \equiv a^2 + (2b - \frac{3}{b})a + \left(\frac{1}{2b} - b\right)^2 > 0$$

which holds if a is outside the roots of the quadratic, that is, if a is not between

$$\frac{3}{2b} - b \pm \sqrt{2}\sqrt{\frac{1}{b^2} - 1}.$$

In particular, if $b > 1$, then Ξ_I is always outside P_2. Let K be the curve defined by

$$a = \frac{3}{2b} - b - \sqrt{2}\sqrt{\frac{1}{b^2} - 1},\ \ 1/2 \leq b \leq 1$$

and

$$a = \frac{3}{2b} - b + \sqrt{2}\sqrt{\frac{1}{b^2} - 1},\ \ 0 \leq b \leq 1.$$

Then $\Xi_I = \Xi_*$ along K. For points (a, b) between I and K, the intersection point Ξ_I lies inside P_2; below I, it lies above P_2 and above K it lies beyond or below P_2. The implication of "beyond" here is that when S_2 emerges from P_2 at Ξ_* and continues, it is, effectively, going backward in time, since movement along it is movement in the direction of decrease of the timelike variable.

Proposition 2.2 *The shocks meet at the wall if $a = b + 1/2b \equiv J(b)$.*

The curve J does not intersect I, but intersects K at the point

$$(a^*, b^*) \equiv \left(\sqrt{1 + \frac{\sqrt{5}}{2}}, \frac{\sqrt{1 + \sqrt{5}}}{2} \right) \tag{2.2}$$

The curve K terminates at this point (since points outside the upper half plane do not have meaning in this problem). A classification of points (a, b) with respect to Ξ_I was given in [9], as follows.

Case 1 The region below I: Ξ_I above P_2.

Case 2 The region above I, below K and left of J: Ξ_I inside P_2, above W.

Case 3 The region above K and left of J: Ξ_I beyond P_2, above W.

Case 4 The region right of J: Ξ_I below W.

See Figure 2.2, where these curves are labelled.

Although Ξ_I is an important point, it may not actually determine the qualitative behavior of the flow since Ξ_I may fail to be admissible. We have the following results.

Proposition 2.3 *In Case 1, Ξ_I is the only admissible primary intersection.*

Proposition 2.4 *In Cases 2, 3, or 4, Ξ_0 is an admissible primary intersection and Ξ_I is not.*

Proof: The entire interior of P_2 is downstream from Ξ_0. In Case 2, all the other primary intersections are inside P_2. ■

In Cases 3 and 4 there may be one or two admissible primary intersections, depending on whether Ξ_A is inside or outside P_2. Noting that Ξ_A is outside P_2 if $\omega_1 \equiv 1/2 + a^2 > 1 + a/b$, we see that Ξ_A is outside P_2 if

$$a > \frac{1}{2b} + \sqrt{\frac{1}{4b^2} + \frac{1}{2}} \equiv L(b).$$

The curve L contains the point (a^*, b^*) and divides Cases 3 and 4 into two subregions, "left" and "right".

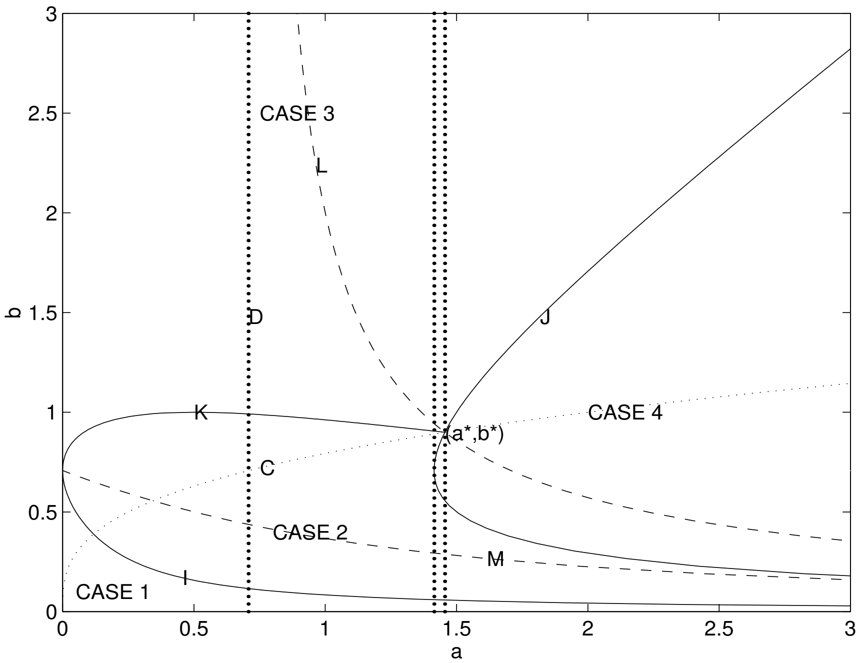

Figure 2.2: Classification of Parameter Space by Position of Ξ_I

Proposition 2.5 *In either Case 3 or Case 4, if* (a, b) *lies to the right of* $a = L(b)$*, there are two admissible primary intersections,* Ξ_0 *and* Ξ_A*. If* (a, b) *lies to the left of this curve, there is only one admissible primary intersection,* Ξ_0*.*

In Case 1, one can construct a Mach reflection solution; in this paper we show how the primary intersections motivate the construction. In this case, the remaining step is to show that a certain degenerate elliptic free-boundary problem has a solution. We have solved the degenerate elliptic problem with a fixed boundary, finding a singular solution in [6] and a regular solution in [8], for different ranges of data. We can use these results to prove the existence of a solution to the free-boundary problem, [4].

To explain the construction of a solution in Case 1 and to obtain preliminary results in the other cases, we next study the quasi-one-dimensional Riemann problems which arise in this problem.

3. Quasi-One-Dimensional Riemann Problems

A quasi-one-dimensional Riemann problem has *data* consisting of a *center* Ξ_0 and two states, U_1, U_2 on a spacelike line, L, through a given point Ξ_0.

The *solution* is defined *downstream* from L. It is a function of

$$t \equiv \frac{\xi - \xi_0}{\eta - \eta_0}$$

defined in a forward half-space below L; it may be useful for the problem at hand only near L.

Now, an acceptable data line

$$L : \qquad (\xi - \xi_0)\cos\theta + (\eta - \eta_0)\sin\theta = 0$$

through (ξ_0, η_0) with normal $\nu = (\cos\theta, \sin\theta) = (\lambda, \mu)$ must have the properties

1. Equation (1.4) is hyperbolic at Ξ_0 and
2. ν is a timelike (co)normal.

For property 1, $\det|A\lambda + B\mu| = 0$ must have two real roots. When (U, Ξ_0) satisfy the condition

$$\xi_0 + \eta_0^2/4 - u > 0 \tag{3.1}$$

then

$$\frac{\mu}{\lambda} = \frac{\eta_0}{2} \pm \sqrt{\frac{\eta_0^2}{4} + \xi_0 - u} \tag{3.2}$$

are the two roots. Thus, to satisfy 1, a pair (U, Ξ_0) must satisfy (3.1). In this case, the two lines through Ξ_0 with normals $(\lambda, \mu)_\pm$ given by (3.2) are the *characteristics*; they are the lines

$$\xi - \xi_0 + \left(\frac{\eta_0}{2} \pm \sqrt{\frac{\eta_0^2}{4} + \xi_0 - u}\right)(\eta - \eta_0) = 0,$$

which are lines through Ξ_0 tangent to the parabola P_u. (This fact was stated in Section 1 and can be seen by a straightforward calculation.)

Definition 3.1 *We say that a pair* (U, Ξ_0) *is a* hyperbolic pair *if condition* (3.1) *holds.*

The characteristics define the limiting slopes for spacelike lines; any straight line through Ξ_0 which does *not* intersect the parabola is spacelike. Furthermore, the side of the line which contains the parabola represents the "future" (forward time). Note that in (3.2) the choice of '+' gives a line tangent to the upper half of the parabola (at a value $\eta > \eta_0$), and the choice '$-$' gives a point of tangency with $\eta < \eta_0$. A spacelike line is hence of the form

$$L : \qquad \xi - \xi_0 + \kappa(\eta - \eta_0) = 0 \text{ with } \left(\frac{\mu}{\lambda}\right)_+ > \kappa > \left(\frac{\mu}{\lambda}\right)_- . \tag{3.3}$$

This line may be vertical but is never horizontal; hence it always has a "left side", which corresponds to the future. A point Ξ belongs to the future if $(\xi - \xi_0, \eta - \eta_0) \cdot (1, \kappa) < 0$; that is, $(1, \kappa)$ is a timelike normal in the *backwards* time direction. This explains property 2.

Now, for Riemann data, we may suppose we are given (U_1, U_2, Ξ_0) with Ξ_0 outside P_i (the parabola corresponding to U_i) for $i = 1, 2$, and a spacelike line L as in (3.3). Since one parabola is inside the other, we need only verify the condition of being spacelike for the parabola with the larger value of u. For definiteness, we define the ordered data triple (U_1, U_2, Ξ_0) to take the value U_1 on the lower half-line $\eta < \eta_0$ and U_2 on the upper.

The *solution* is a function

$$U(t) \equiv U\left(\frac{\xi - \xi_0}{\eta - \eta_0}\right)$$

defined in the *future*; that is, for

$$\xi - \xi_0 + \kappa(\eta - \eta_0) \equiv (t + \kappa)(\eta - \eta_0) \leq 0.$$

If we describe the solution to the Riemann problem by beginning at $t = -\kappa$ and $U = U_1$ on L, then t increases to infinity (horizontal line) and then continues with t increasing from $-\infty$ to $-\kappa$ again; at the final point, $U = U_2$ on L. This parameterization of the solution may appear somewhat awkward; however, the solution is always constant in a neighborhood of $t \to \pm\infty$.

Our aim is to describe the solution to the Riemann problem for all data. Now, at any t, $U(t)$ either

1. is constant in a neighborhood of t or

2. has a shock at t or

3. has a rarefaction in a (possibly one-sided) neighborhood of t.

Item 1 needs no explanation. We next describe shocks and rarefactions in turn.

3.1 The Shock Polar

If there is a shock on the line $\xi - \xi_0 = t(\eta - \eta_0)$, then from (1.5) we have the *Rankine-Hugoniot relation*:

$$F(U, \Xi_0) - F(U_0, \Xi_0) = t(G(U, \Xi_0) - G(U_0, \Xi_0))$$

where U and U_0 are the constant states on either side of the discontinuity. Letting $[v] = v - v_0$ and so on, we have

$$\begin{aligned} \frac{1}{2}[u^2] - \xi_0[u] - t[v] + t\eta_0[u] &= 0 \\ -[v] - t[u] &= 0 \end{aligned}$$

so, immediately,

$$t = -\frac{v - v_0}{u - u_0} = -\frac{[v]}{[u]}; \qquad [v] = -[u]t. \tag{3.4}$$

Eliminating t from the other equation, we get

$$\frac{[v]}{[u]} = \frac{\eta_0}{2} \pm \sqrt{\frac{\eta_0^2}{4} + \xi_0 - \left(\frac{u + u_0}{2}\right)}. \tag{3.5}$$

For (3.5) to have real solutions, we see that at least one of (U, Ξ_0) and (U_0, Ξ_0) must be a hyperbolic pair. Assuming that (U_0, Ξ_0) is hyperbolic, then (3.5) defines the *shock polar*; it is defined for

$$u \leq 2\left(\frac{\eta_0^2}{4} + \xi_0\right) - u_0 \equiv u_M; \tag{3.6}$$

and always forms a loop; there are two values of v for each $u \neq u_0$, u_M, and those values are distributed above and below the line

$$\frac{[v]}{[u]} = \frac{\eta_0}{2},$$

which has positive slope if $\eta_0 > 0$. We denote the branches by $S^\pm$. The shock polar is also defined for pairs (U_0, Ξ_0) which are not hyperbolic, but then it is not a loop; in this case $u_M < u_0$, and the locus consists of a single smooth branch and the isolated point U_0. See Figure 3.1.

To describe the shock polar, we introduce the following conventions. Fix Ξ_0 and U_0 so that (U_0, Ξ_0) is a hyperbolic pair. Define the rightmost state on the shock polar:

$$U_M = (u_M, v_M) \equiv \left(2\left(\frac{\eta_0^2}{4} + \xi_0\right) - u_0, v_0 + \eta_0\left(\frac{\eta_0^2}{4} + \xi_0 - u_0\right)\right).$$

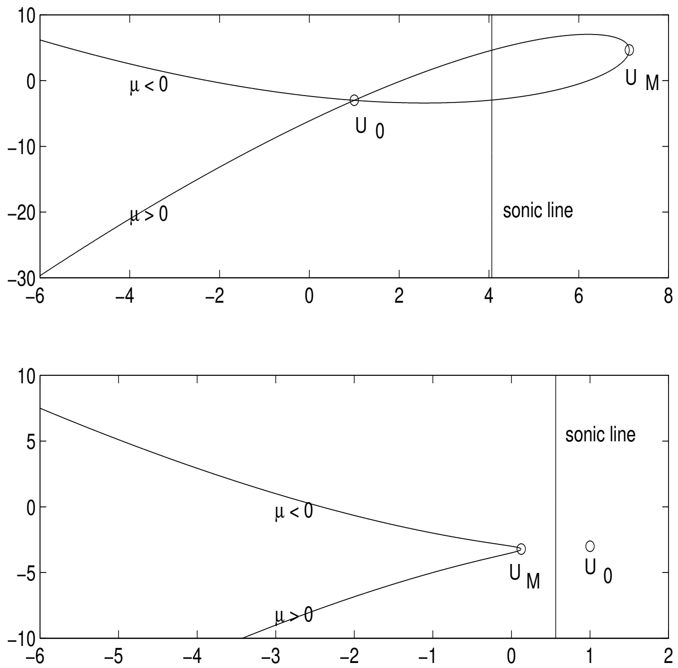

Figure 3.1: Shock Polar Configurations for $U_0 = (1, -3)$ and $\Xi_0 = (2.5, 2.5)$ (top) and for $U_0 = (1, -3)$ and $\Xi_0 = (0.5, 0.5)$ (bottom)

Define the parameter μ to be distance along the shock polar path from U_M, taken negative or positive according to the following convention:

$$\begin{cases} \mu < 0 \;\; (S^+): & \frac{[v]}{[u]} = \frac{\eta_0}{2} - \sqrt{\frac{\eta_0^2}{4} + \xi_0 - \frac{u+u_0}{2}} \\ \mu > 0 \;\; (S^-): & \frac{[v]}{[u]} = \frac{\eta_0}{2} + \sqrt{\frac{\eta_0^2}{4} + \xi_0 - \frac{u+u_0}{2}}. \end{cases} \tag{3.7}$$

Thus, $\mathrm{sgn}(du/d\mu) = -\mathrm{sgn}\mu$. As $\mu \to -\infty$, $[v]/[u] \to -\infty$ and as $\mu \to \infty$, $[v]/[u] \to \infty$. If t denotes the shock angle[1] of the shock between U and U_0, then

$$\begin{cases} \mu < 0 \;\; (S^+): & t = -\frac{\eta_0}{2} + \sqrt{\frac{\eta_0^2}{4} + \xi_0 - \frac{u+u_0}{2}} \\ \mu > 0 \;\; (S^-): & t = -\frac{\eta_0}{2} - \sqrt{\frac{\eta_0^2}{4} + \xi_0 - \frac{u+u_0}{2}}. \end{cases} \tag{3.8}$$

Note that

$$\frac{dt}{du} = \begin{cases} -\frac{1}{4}\left(\frac{\eta_0^2}{4} + \xi_0 - \frac{u+u_0}{2}\right)^{-1/2}, & \mu < 0 \\ \frac{1}{4}\left(\frac{\eta_0^2}{4} + \xi_0 - \frac{u+u_0}{2}\right)^{-1/2}, & \mu > 0 \end{cases}$$

[1] We refer to t as a 'shock angle' throughout. It is actually the cotangent of the angle of the shock line to the horizontal.

and so $dt/d\mu < 0$ for all μ. We use the following notation for the local characteristic angles:

$$\frac{\xi - \xi_0}{\eta - \eta_0} = -\left(\frac{\mu}{\lambda}\right)(U) \equiv \tau(U)$$

with

$$\tau_+(U) \equiv -\frac{\eta_0}{2} + \sqrt{\frac{\eta_0^2}{4} + \xi_0 - u} > -\frac{\eta_0}{2} - \sqrt{\frac{\eta_0^2}{4} + \xi_0 - u} \equiv \tau_-(U).$$

Note that the τ_- characteristic is tangent to the parabola *above* $\eta = \eta_0$, and the τ_+ characteristic is tangent below (as illustrated in Figure 1.2). It is useful to define the *sonic points*. Let u_s be the *sonic value*, where $\tau_\pm(U)$ becomes complex:

$$u_s = \frac{\eta_0^2}{4} + \xi_0$$

and note that $u_0 < u_s < u_M$; in fact,

$$u_M - u_s = \frac{\eta_0^2}{4} + \xi_0 - u_0 = u_s - u_0.$$

There are two sonic points, $U_{s\pm}$, on the shock polar, corresponding to μ positive or negative. Let $\mu_1 < \mu_2 < \mu_3 = 0 < \mu_4 < \mu_5$ be the values of μ corresponding to U_0 (μ_1 and μ_5), U_s (μ_2 and μ_4) and U_M (μ_3). If we sketch all the quantities on a single graph, Figure 3.2, it is easy to see what types of shocks appear, and where.

The standard Lax geometric admissibility condition implies that t in (3.8) must be between $\tau_+(U)$ and $\tau_+(U_0)$ for a $+$-shock (below the parabola) and between $\tau_-(U)$ and $\tau_-(U_0)$ for a $-$-shock (above); in addition *transonic* shocks are admissible if U_0 (the state with real characteristics) is upstream. Discussion of these admissibility conditions can be found in [5]. The state with the smaller value of u is always upstream (on the right side of the shock, away from the smaller parabola). It is straightforward to check that in physical (ξ, η) space, the shock line $t = (\xi - \xi_0)/(\eta - \eta_0)$ always intersects the outer parabola twice and is bounded away from the inner one.

For each value of μ there is a single admissible shock configuration, consisting of the triple (U, U_0, t) (note this is all with respect to a fixed Ξ_0), and there are five intervals of qualitatively different behavior. They are

1. $\mu \in (-\infty, \mu_1)$: $\tau_+(U) > t > \tau_+(U_0)$; shock is *below* parabola P_u and U is *upstream.*

2. $\mu \in (\mu_1, \mu_2)$: $\tau_+(U_0) > t > \tau_+(U)$; shock is *below* parabola P_0 and U_0 is *upstream.*

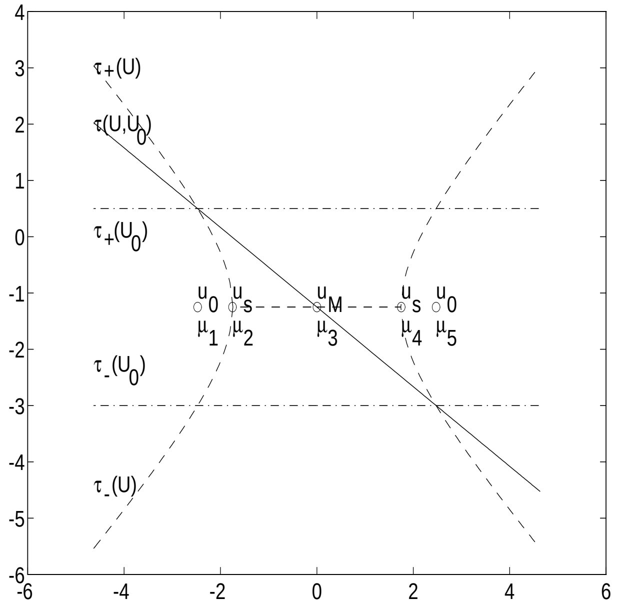

Figure 3.2: Characteristic and Shock Angles on Shock Polar for $U_0 = (1, -3), \Xi_0 = (2.5, 2.5)$

3. $\mu \in (\mu_2, \mu_4)$: $\tau_+(U_0) > t > \tau_-(U_0)$; $\tau_\pm(U)$ complex; U_0 is *upstream* and shock is transonic: neither above nor below; Ξ_0 is inside P_u.

4. $\mu \in (\mu_4, \mu_5)$: $\tau_-(U) > t > \tau_-(U_0)$; shock is *above* parabola P_0 and U_0 is *upstream.*

5. $\mu \in (\mu_5, \infty)$: $\tau_-(U_0) > t > \tau_-(U)$; shock is *above* parabola P_u and U is *upstream.*

An example from each of intervals 1 through 4 is sketched in Figure 3.3.

To use this information to solve quasi-one-dimensional Riemann problems with data U_1 and U_2 on L, note that the given states U_1 and U_2 must both be *upstream* states with respect to a shock joining them to adjacent states. Also, typically, the shock between U_1 and an adjacent state will be a $+$-shock (below the parabola: in interval 2 or 3) and that between U_2 and an adjacent state a $-$-shock (above: in interval 3 or 4). The 2-interval from U_1 will not intersect the 4-interval from U_2, unless U_1 and U_2 are correctly positioned relative to each other in the u, v plane: U_1 must be more or less above U_2 and not too far away. Generally, the shock polars from U_1 and U_2 will intersect twice, so the intermediate state is not uniquely defined from the data. It is also clear that one case of interest, with Riemann data the

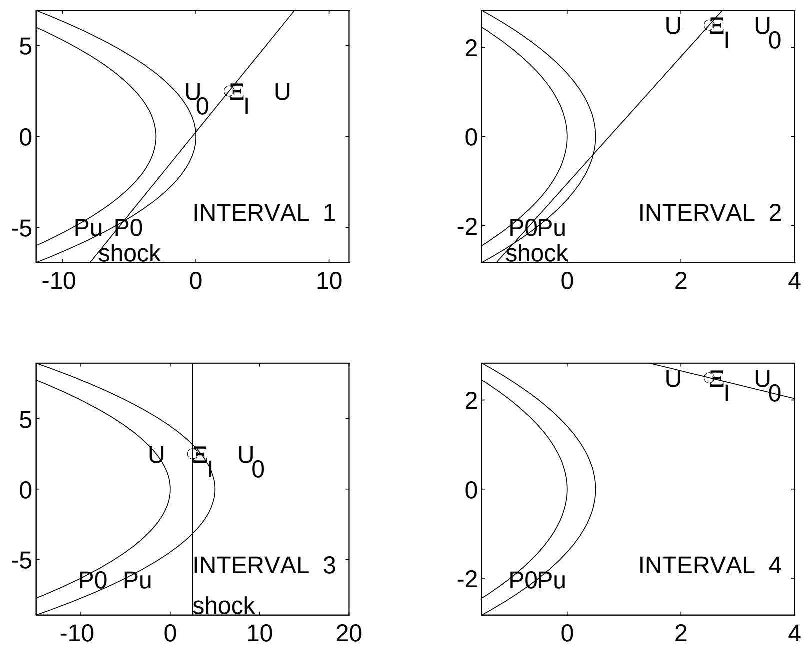

Figure 3.3: Admissible Configurations Along the Shock Polar

states U_0 and U_2 given by the original data, is not of this type, and the solution of this Riemann problem must also include rarefaction waves, which we now discuss.

3.2 The Rarefaction Polar

Centered simple waves are the third type of local solution $U(t)$ introduced at the beginning of Section 3. From (1.4) we obtain

$$(A - tB)U' = 0; \tag{3.9}$$

where now $' = d/dt$. Hence,

$$t = -\left(\frac{\mu}{\lambda}\right)_{\pm} \equiv \tau_{\mp}(U) = -\frac{\eta}{2} \mp \sqrt{\frac{\eta^2}{4} + \xi - u} = -\frac{\eta_0}{2} \mp \sqrt{\frac{\eta_0^2}{4} + \xi_0 - u},$$

where replacement of Ξ in the formula by Ξ_0 is justified since the characteristic through Ξ also goes through Ξ_0. Now U' is a null vector of (3.9), so one finds (using the definitions of A and B in (1.4)) $tu' + v' = 0$ or

$$\frac{dv}{du} = -t = \frac{\eta_0}{2} \pm \sqrt{\frac{\eta_0^2}{4} + \xi_0 - u} = -\tau_{\mp}$$

(for the rarefaction curve corresponding to $\tau_\mp$), which we can integrate:

$$v(u) = \frac{\eta_0}{2}u \mp \frac{2}{3}\left(\frac{\eta_0^2}{4} + \xi_0 - u\right)^{3/2} + c$$

for the rarefaction curves through Ξ_0. Note that

$$\frac{dt}{du} = \pm\frac{1}{2}\frac{1}{\sqrt{\frac{\eta_0^2}{4} + \xi_0 - u}}$$

(the + sign refers to the τ_- root) and is positive for the τ_- root, and negative for the τ_+ root.

We define $R(U_0, \Xi_0)$, the *rarefaction polar* connecting to U_0, centered at Ξ_0, by the formula

$$v = v_0 + \frac{\eta_0}{2}(u - u_0) \mp \frac{2}{3}\left\{\left(\frac{\eta_0^2}{4} + \xi_0 - u\right)^{3/2} - \left(\frac{\eta_0^2}{4} + \xi_0 - u_0\right)^{3/2}\right\}. \tag{3.10}$$

(The $-$ sign defines R^-, corresponding to τ_-, the + sign gives R^+, corresponding to τ_+.) Both U and U_0 must be hyperbolic at Ξ_0, and the curves are defined for $u \leq u_s = \eta_0^2/4 + \xi_0$. Unlike the shock polar, the rarefaction polar does not form a loop, but has two finite and two semi-infinite branches. For a sketch of the rarefaction curves, see Figure 3.4.

A picture of the local characteristic angles along $R(U_0, \Xi_0)$ (see Figure 3.5) can be used to construct a rarefaction wave configuration, as in Figure 3.6. There are four cases:

1. For an R^- wave, $\tau_-(u) < \tau_-(u_0)$ if U_0 is the upstream state. Hence, the semi-infinite branch of R^-, with $u < u_0$, consists of states to which U_0 can be joined by a rarefaction, with U_0 the upstream state.

2. The other part of R^-, with $u_0 < u < u_s$, consists of τ_- waves where U_0 is now the downstream state.

3. On the τ_+ branch, the rarefactions are tangent to the lower branches of the parabolas (as in Figure 3.6); again, the semi-infinite branch, $u < u_0$, contains states which are downstream from U_0.

4. On the part of R^+ with $u_0 < u < u_s$, U is the upstream state (the case pictured in Figure 3.6).

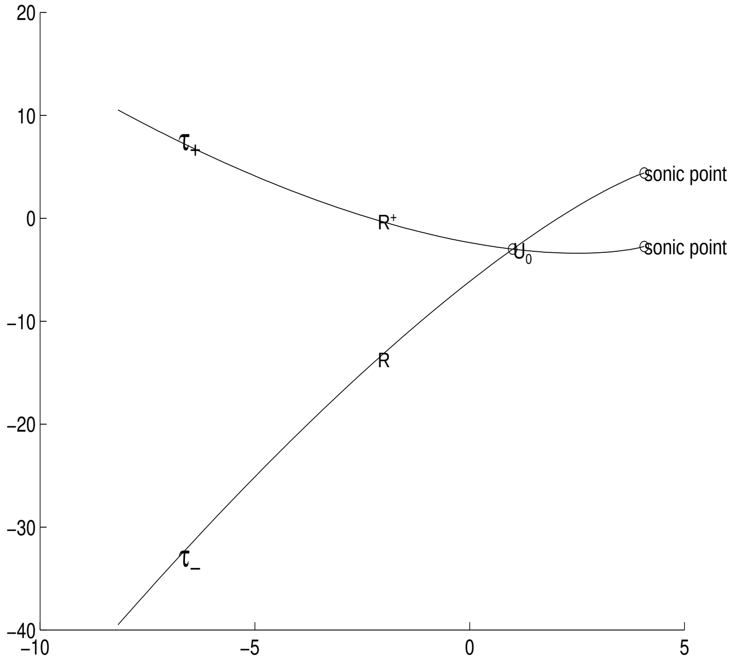

Figure 3.4: The Rarefaction Polar at $U_0 = (1, -3); \Xi_0 = (2.5, 2.5)$

3.3 Solvable Quasi-One-Dimensional Riemann Problems

Unlike the standard one-dimensional Riemann problem, quasi-one-dimensional Riemann problems do not have solutions for all choices of U_1, U_2, and Ξ_0. Nor will the solution always be uniquely defined. However, we can give a precise result as follows.

Define the *downstream wave locus*, $D(U_1)$, of a state U_1, with respect to a fixed Ξ_0, as the union of all states which can be joined to U_1 by a shock or rarefaction in which U_1 is the upstream state. This locus is defined only if U_1 is a hyperbolic state. It consists of the loop part of the shock polar (intervals 2, 3, and 4), and the semi-infinite line segments from the rarefaction polar (intervals 1 and 3). Qualitatively, it looks like the shock polar; in particular, it extends beyond the line $u = u_s$. See Figure 3.7.

The downstream wave locus divides the half-plane $u \leq u_s$ into four regions, labelled 1 – 4 in Figure 3.7; we label the region above U_1 as '1' and continue counterclockwise. We can prove

Theorem 3.1 *Given a Riemann data triple (U_1, U_2, Ξ_0) with hyperbolic states U_1 on the lower half and U_2 on the upper half of a spacelike line L through Ξ_0; let $D(U_1)$ be the downstream wave locus of U_1. Then if U_2*

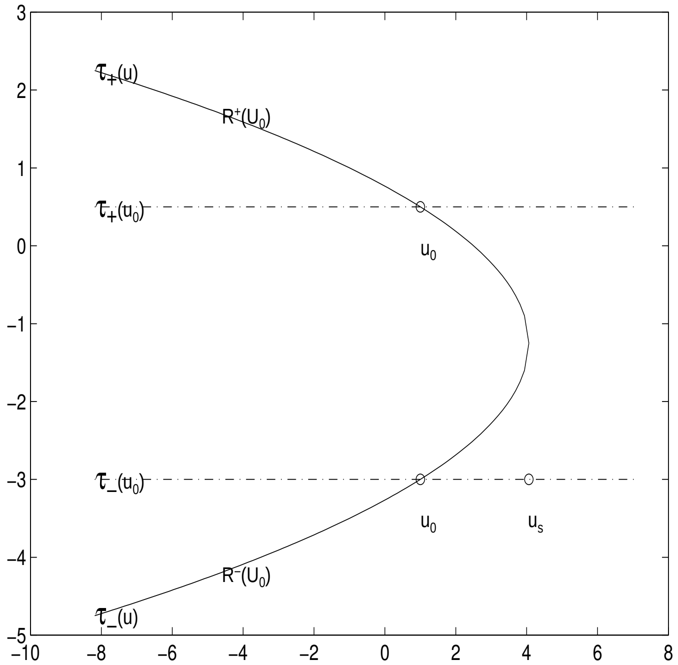

Figure 3.5: Characteristic Angles on the Rarefaction Polar for $U_0 = (1, -3), \Xi_0 = (2.5, 2.5)$

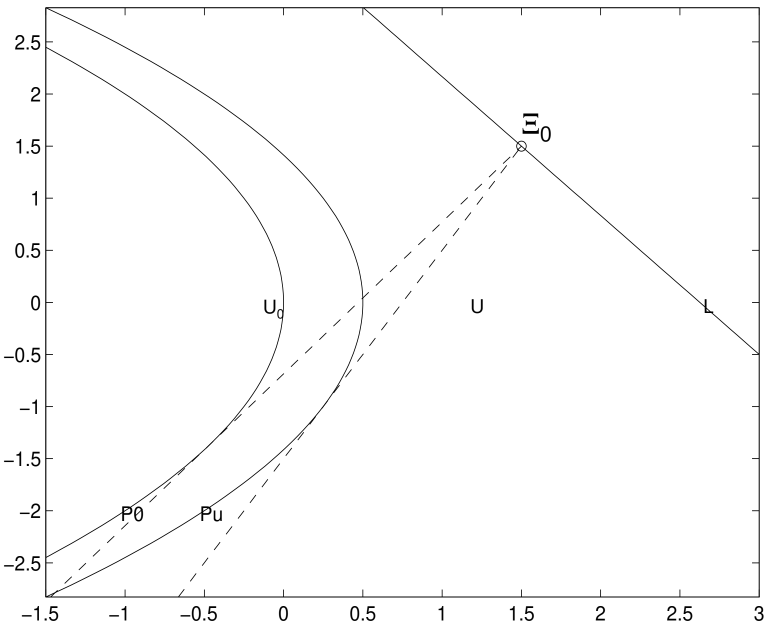

Figure 3.6: A Centered Rarefaction Wave

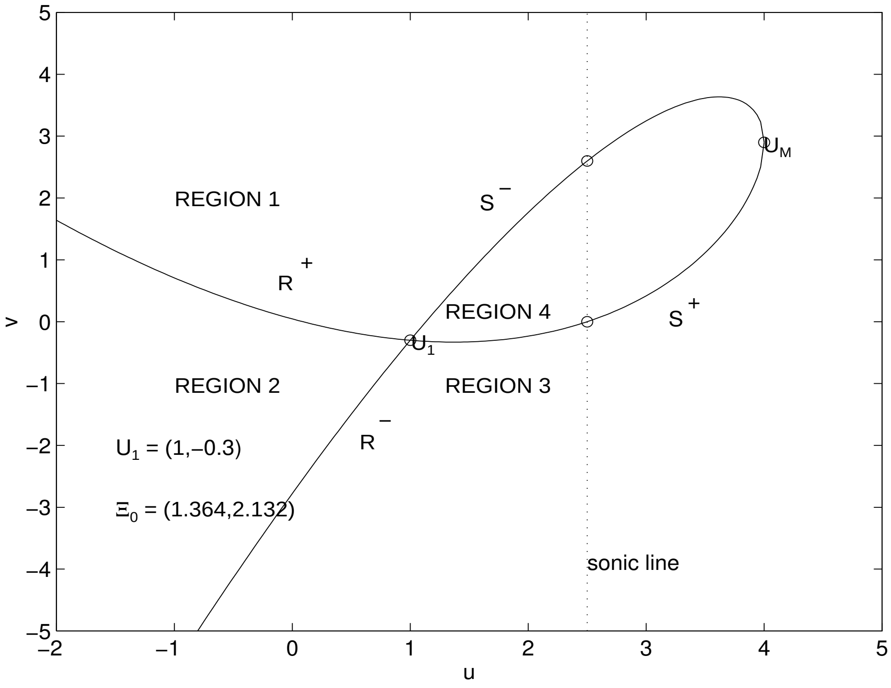

Figure 3.7: Downstream Locus and Solution Regions of Quasi-One-Dimensional Problems

lies in any of the regions 1, 2, or 4 in the complement of $D(U_1)$*, the Riemann problem has a unique admissible solution. If* U_2 *lies in region 3, there may be none, one or two admissible solutions.*

Proof: An admissible solution is a state U_m on the intersection of $D(U_1)$ and $D(U_2)$ with the property that the wave angles are compatible with construction of a wave between U_1 and U_m and another between U_2 and U_m. It is useful, in visualizing what points on the shock and rarefaction polars are associated with particular angles, to note that the equation $[v] = -[u]t$, (3.4), means that the shock angle, t, is orthogonal to the line segment joining U_1 to U on $D(U_1)$ (for rarefactions, the corresponding equation is $dv/du = -t$, relating the wave angle to the tangent to the rarefaction polar). The fact that there are no horizontal waves corresponds to the nonexistence of vertical tangents or secants to the polars.

The three feasibility conditions on the angles t_i of the waves between U_i and U_m $(i = 1, 2)$ are

$$t_1 > \tau_-(U_1), \;\; t_2 < \tau_+(U_2), \;\; \frac{1}{t_1} > \frac{1}{t_2}.$$

The first implies that U_m is not on $R^-(U_1)$, the second that U_m cannot be on $R^+(U_2)$. The third says that, with respect to U_m, four configurations of U_1 and U_2 are possible:

I. U_1 is left of U_m and U_2 is also left of U_m and below the line segment joining U_m and U_1.

II. U_1 is left of U_m and U_2 is right of U_m and above the extension of the line segment joining U_m and U_1.

III. U_1 is right of U_m and U_2 is also right of U_m and above the line segment joining U_m and U_1.

IV. U_1 is right of U_m and U_2 is left of U_m and below the extension of the line segment joining U_m and U_1.

All other arrangements are inadmissible.

Now, suppose U_2 is in region 1. We invoke standard theorems of ordinary differential equations to tell us that the R^+ and R^- curves form smooth vector fields which cover the left half-plane without self-intersections; curves from opposite families intersect uniquely and transversely. A calculation, or use of a general result on convex shock curves, also tells us that intersections of shock loops with each other and with rarefaction curves are governed by exactly the mechanism one would see if the downstream locus were simply translated. Hence, when U_2 is in region 1 of Figure 3.7, there may be some intersections of shock curves, all of which are inadmissible, and there is always an intersection of $R^+(U_1)$ with $R^-(U_2)$; this produces a unique admissible point U_m and a solution consisting of a pair of rarefaction waves.

If U_2 is in region 2, the unique admissible intermediate state U_m is at the intersection of $R^+(U_1)$ and $S^-(U_2)$. This intersection always exists if U_2 is in region 2, for the shock loop of U_1 is inside the shock loop of U_2.

In region 4, which is bounded, the unique solution is the intersection of $R^-(U_2)$ and $S^+(U_1)$. This solution is illustrated in Figure 3.8.

However, in region 3, the only admissible points are the intersection of the shock loops $S(U_1)$ and $S(U_2)$. These points are the simultaneous solution, with $u_m > u_i$, of

$$\frac{v_m - v_1}{u_m - u_1} = \frac{\eta_0}{2} - \sqrt{\frac{\eta_0^2}{4} + \xi_0 - \left(\frac{u_m + u_1}{2}\right)}$$

(see equation (3.5)) and

$$\frac{v_m - v_2}{u_m - u_2} = \frac{\eta_0}{2} + \sqrt{\frac{\eta_0^2}{4} + \xi_0 - \left(\frac{u_m + u_2}{2}\right)}.$$

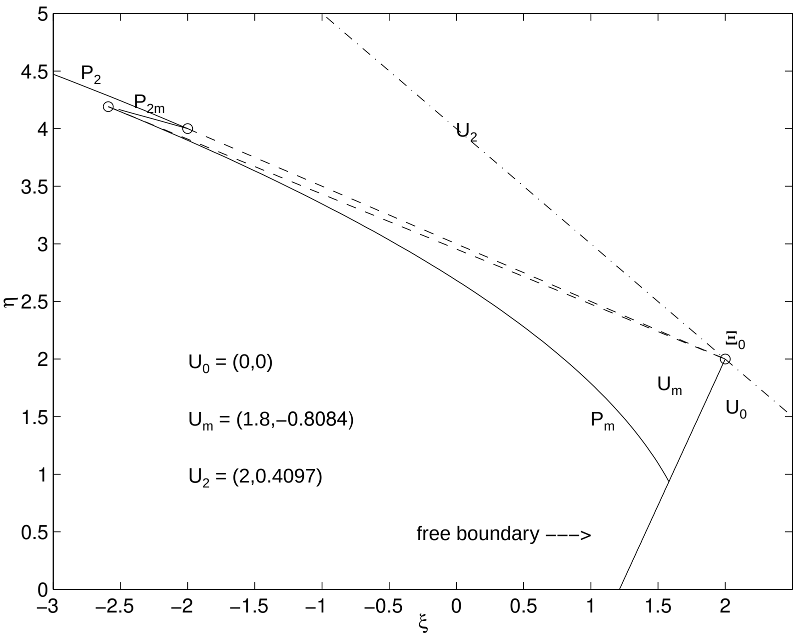

Figure 3.8: Riemann Solution for U_2 in Region Four and Boundary of the Subsonic Region

For fixed u_1 and u_2, if $v_1 - v_2$ is too large, there will not be a solution. Furthermore, except along a curve separating the region of no solutions, there will be two solutions. Again, typically, though not always, one solution will be supersonic and one subsonic. Standard admissibility criteria show that both are admissible. ∎

3.4 The Hyperbolic Solution for Case 1 Parameters

Theorem 3.1 establishes the form of the solution of the hyperbolic Riemann problem which occurs when (a, b) lies below the curve I (Case 1 data).

Theorem 3.2 *If oblique shock data* (1.2) *given for equation* (1.1) *are such that $a \leq I(b)$, then a hyperbolic quasi-one-dimensional Riemann problem occurs at Ξ_I. Furthermore, the data for this problem lead to a region 4 configuration, and there is a unique admissible solution, which consists of a rarefaction wave and a shock.*

Proof: The Riemann problem has data U_0 below Ξ_I and U_2 above; here for L we take any spacelike line. Because Ξ_I is outside P_2 by hypothesis, the Riemann data is hyperbolic. Now, $U_2 = (1 + a/b, 0)$ lies directly to the right of $U_0 = (0,0)$. We claim that this point is in region 4. Because of the remarks following equation (3.6), it is in either region 3 or 4, and it is in region 4 if the curve $S^+(U_0)$ lies below the u-axis at $u = u_2$. But on $S^+(U_0)$, from (3.5),

$$v = u\left(\frac{\eta_I}{2} - \sqrt{\frac{\eta_I^2}{4} + \xi_I - \frac{u}{2}}\right) \tag{3.11}$$

and $v(u_2) < 0$ if $\xi_I > u_2/2$. Checking the value of ξ_I in Table 2.1 shows that this is indeed the case.

This construction can also be used to estimate the values of v_m and u_m. We find $\xi_I - u_2/2 = a/2b$. This can be made arbitrarily small, and hence $v(u_2)$ in equation (3.11) arbitrarily close to zero, by choosing a small relative to b. Then $R^-(U_2)$ will intersect $S^+(U_0)$ very close to U_2 (it can be checked that the slope of $R^-(U_2)$ is of order unity in this case); that is, v_m is negative and near zero, while u_m is less than u_2 and very close to u_2. ■

In fact, this solution gives a solution to the shock interaction problem at every point in the (ξ, η) plane which is supersonic. We have

Theorem 3.3 *The Riemann problem (1.2) for the unsteady transonic small disturbance equation (1.1) has a solution consisting of shocks, constant states and centered rarefaction waves in the exterior of the parabola P_m, defining the elliptic region for the state U_m, if the data (a, b) are of Case 1 type.*

Proof: The solution outside P_m is constructed by continuing the rarefaction wave joining U_2 to U_m out to infinity, and then letting $U = U_m$ be constant below the rarefaction and between the rarefaction and the shock, outside P_m. When the shock enters P_m it is expected to bend; inside P_m one can formulate a problem for (1.1) which is elliptic inside the region and degenerate elliptic on the boundary. Data along the ξ axis are chosen to be symmetric: $u_\eta = 0 = v$. The continuation of the shock, satisfying the Rankine-Hugoniot condition and with the constant state U_0 upstream, leads to a free-boundary problem. ■

The degenerate elliptic problem is solved in [8] and [6] and we are currently studying the free-boundary problem, [4].

The solution constructed this way is not unique, even in the hyperbolic region, since we continued the rarefaction fan beyond the parabolas. This violates causality: the infinite rays extend in the backwards timelike direction. An alternative and more physical construction terminates each ray in the rarefaction fan at the point where it becomes sonic. Then it becomes necessary, to complete the problem, to find the nonuniform subsonic solution in the strip between P_2 and P_m. This changes the degenerate part of the boundary in the free-boundary problem mentioned above. The free-boundary problem for the position of the transonic shock between the upstream state U_0 and a subsonic state U remains the same, but the region is now bounded by a part of the sonic parabola P_2, a part of the sonic parabola P_m, the wall, and a sonic curve P_{2m} along which the states in the rarefaction wave between U_2 and U_m become sonic. If (ξ_I, η_I) denote the coordinates of Ξ_I, the equation for the curve P_{2m} is given by

$$\xi - \xi_I = \frac{\eta}{2}(\eta_I - \eta). \tag{3.12}$$

Figure 3.8 pictures the corresponding hyperbolic solution and the boundary components for the elliptic problem. Equation (1.1) is elliptic inside the region where the flow is subsonic, and degenerate on the boundary $P_2 \cup P_m \cup P_{2m}$. We have not yet attempted to solve this problem for two reasons. First, we wish to understand the degenerate free-boundary problem, and so we have chosen a simplified problem to solve. In addition, P_m is close to P_2, so this ambiguous region is small, and should not affect the existence of the solution in the interesting region near the free boundary. (However, to describe some more complicated wave interactions, as we outline in Section 4, we assume this more physical problem has a solution as well.)

A second reason for not considering the details of the problem near the tail of the parabola is that, as mentioned at the beginning of the paper, the original problem is not hyperbolic in time, and the ill-posedness centers about the treatment of the negative ξ-axis. If we were to consider, instead of (1.1), a problem such as the nonlinear wave equation, the nature of the difficulty in this region (now confined to a finite part of the plane) becomes clearer, and needs to be analysed.

We conclude this section with a remark about the wave interaction which occurs in the limit of Case 1, when (a, b) lies on the curve I.

Remark: (The Hyperbolic Solution for $(a, b) \in I$) In this case $\Xi_I = \Xi_0 = \Xi_1$ and this is a limiting case in which Ξ_I is still an admissible primary intersection. The shock S_2 is sonic at Ξ_I and so we call the interaction between S_1 and S_2 at Ξ_I a *degenerate hyperbolic wave interaction.* We solve this degenerate hyperbolic problem in the same way as for Case 1 data. By Theorem 3.2, the data for this problem leads to a region 4 configuration of wave curves and the solution consists of a $-$-rarefaction wave from U_2 to a state U_m with $u_2 > u_m$, followed by a $+$-shock between U_m and U_0.

In the more physical solution (where the characteristics in the rarefaction fan terminate at the sonic points), the rarefaction wave consists of characteristics whose lengths decrease to zero as $u \to u_2$.

To complete the solution we again need to solve a free-boundary problem for the position of the transonic shock between U_0 and the subsonic state U in the domain whose boundary has the same constituents as in Case 1 data. The degenerate boundary consists of the parabola P_2, the curve P_{2m}, given by equation (3.12), along which the rarefaction wave is sonic, and the parabola P_m across which U_m changes from supersonic to subsonic. Even in this degenerate case, the component P_{2m} of the degenerate boundary where U is nonconstant is not adjacent to the free boundary.

4. Shock Reflection Problems for Other Parameter Values

In the preceding section, we showed how the problem of Mach stem formation reduces to a hyperbolic Riemann problem when the initial shocks at infinity fall into Case 1 (this is the case of almost vertical shocks). The quasi-steady problem in this particularly straightforward case is simplified by the fact that Ξ_I is an admissible primary intersection; in fact, it is the only one, and it organizes the entire problem.

Outside this case, the behavior at Ξ_I does not determine the problem; in fact, Ξ_I may not even occur. There are four other modes of shock interaction which we can set up in some regions of space (possibly overlapping). We have not yet solved the corresponding elliptic problems for these cases, but we formulate them here, leaving the rest of the investigation to the future.

We begin by discussing another shock reflection problem, which may be hyperbolic, and may be primary, for some values of a and b. We recall that Proposition 5 shows that Ξ_A is a primary intersection if (a, b) lies to the right of the curve $L(b)$ in Figure 2.2.

4.1 Symmetric Shock Reflection at the Wall

The interaction of the incident shock, S_1, with the wall may be reduced to a standard Riemann problem by considering as Riemann data at $\Xi_A = (\omega_1, 0)$ a spacelike line L (a vertical line through Ξ_A) and data U_1 on the upper half of the line and the reflected state $U_1^* \equiv (1, a)$ on the lower half.

Proposition 4.1 *This is a hyperbolic problem if* $a \geq 1/\sqrt{2}$.

Proof: The states U_1 and U_1^* are hyperbolic at Ξ_A if $u_1 = 1 \leq \xi_A = \omega_1$, or $a^2 \geq 1/2$. ■

However, for data of this form, if we consider the downstream locus, $D(U_1^*)$, for the value on the lower half-line, then U_1 is in region 3 of Theorem 3.1, where we are not guaranteed existence or uniqueness of a solution. For the simple, symmetric data we consider here, the condition for existence is easy to derive. In fact, we have

Proposition 4.2 *The quasi-one-dimensional Riemann problem with the data triple* (U_1^*, U_1, Ξ_A) *has a solution if and only if* $a \geq \sqrt{2}$*. If* $a > \sqrt{2}$*, there are two solutions:*

$$U_R = (1 + a^2 - a\sqrt{a^2 - 2}, 0) \tag{4.1}$$

$$U_F = (1 + a^2 + a\sqrt{a^2 - 2}, 0). \tag{4.2}$$

Proof: The shock polar of U_1 has the equation (from (3.5))

$$\frac{v + a}{u - 1} = \pm\sqrt{\frac{1}{2} + a^2 - \frac{u + 1}{2}} \tag{4.3}$$

and by symmetry the solution to the Riemann problem must have an intermediate state with $v = 0$. Solving for u we find (eliminating the solution $u = 0$)

$$u = 1 + a^2 \pm a\sqrt{a^2 - 2}$$

from which we get (4.1) and (4.2). ■

The intermediate state is hyperbolic if $u < \xi_A \equiv \frac{1}{2} + a^2$. Hence U_F is never hyperbolic, while U_R is hyperbolic if

$$a \geq \left(1 + \frac{\sqrt{5}}{2}\right)^{\frac{1}{2}} \equiv a^*$$

where a^* is identified in equation (2.2). Since $a^* > \sqrt{2}$, there is a narrow range of a in which both solutions (4.1) and (4.2) are elliptic (subsonic at Ξ_A); for larger a, only the state with larger magnitude is elliptic.

Let us identify the shock between U_1 and U_R by the name S_R (R stands for 'reflected'; F will stand for 'fast reflected' in (4.2)). The shock has the equation

$$\xi = \kappa_R \eta + \omega_R, \text{ where } \omega_R = \xi_A = \frac{1}{2} + a^2 \text{ and } \kappa_R = -\frac{1}{a - \sqrt{a^2 - 2}}.$$

Similarly, the shock between U_1 and U_F is S_F, with

$$\xi = \kappa_F \eta + \omega_F, \text{ where } \omega_F = \xi_A = \frac{1}{2} + a^2 \text{ and } \kappa_F = -\frac{1}{a + \sqrt{a^2 - 2}}.$$

We now formulate the perturbed regular reflection equations. These equations can be formulated for all $a \geq \sqrt{2}$ and $a > I(b)$. We shall call this region of parameter space $\mathcal{R}$. We note that only if $a > L(b)$ is Ξ_A an admissible primary intersection, but that it is always *locally admissible* in $\mathcal{R}$: that is, it lies outside of and upstream from P_1.

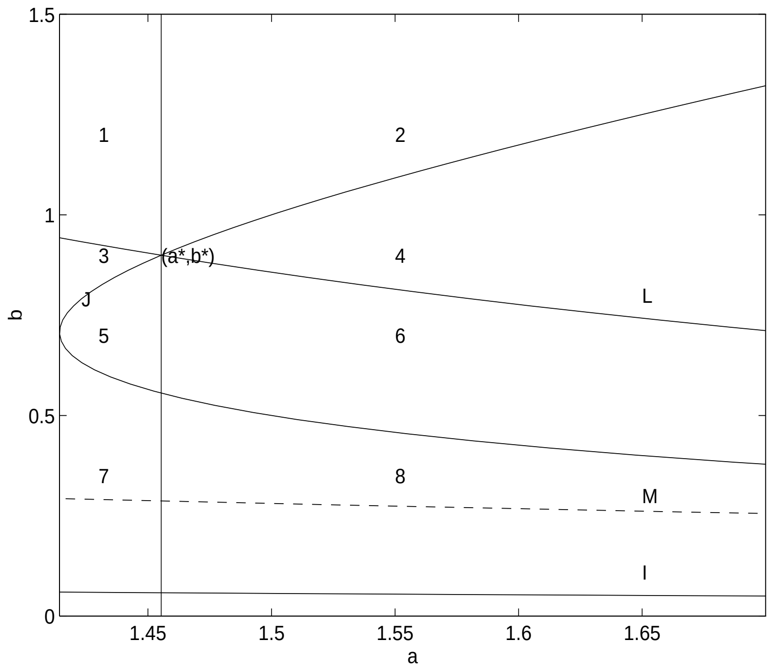

Figure 4.1: Subregions of the Regular Reflection Region, $\mathcal{R}$

Proposition 4.3 *The curve $J(b)$ divides $\mathcal{R}$ into three regions:*
top: $b > 1/(a - \sqrt{a^2 - 2})$, *and* $u_2 < u_R < u_F$
middle: $1/(a - \sqrt{a^2 - 2}) > b > 1/(a + \sqrt{a^2 - 2})$, *and* $u_R < u_2 < u_F$
bottom: $b < 1/(a + \sqrt{a^2 - 2})$, *and* $u_R < u_F < u_2$.
On the boundaries, we have

$$b = \frac{1}{a - \sqrt{a^2 - 2}}, \exists \text{ uniform solution } U_2 = U_R, S_2 = S_R \tag{4.4}$$

$$b = \frac{1}{a + \sqrt{a^2 - 2}}, \exists \text{ uniform solution } U_2 = U_F, S_2 = S_F. \tag{4.5}$$

The line $a = a^*$ and the curve $a = L(b)$ also demarcate regions of potentially different behavior in $\mathcal{R}$. These three curves divide $\mathcal{R}$ into eight subregions, as shown in Figure 4.1.

For reference, we also draw a diagram of the uniform reflected shock solutions on the boundaries, using (4.4) and (4.5). The important point is to note where the boundaries of the super- and subsonic regions lie, since this is where perturbed solutions are expected to become nonuniform. See

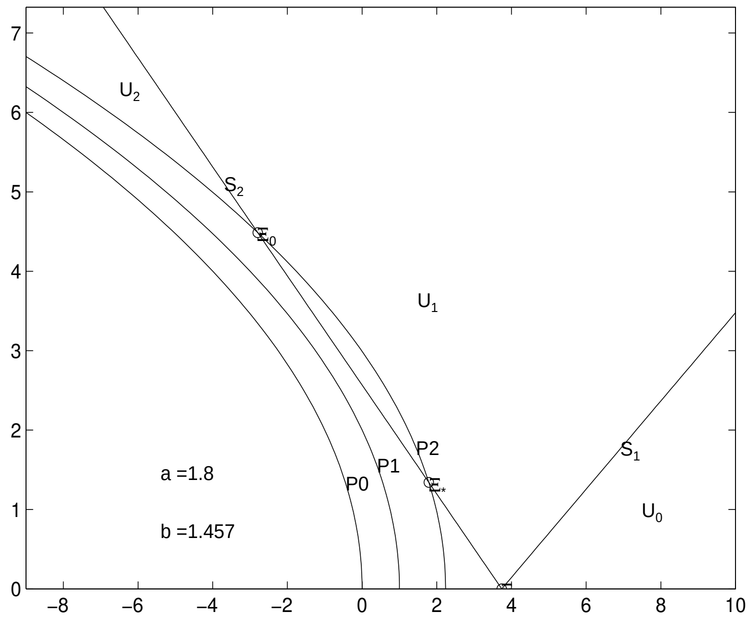

Figure 4.2: Uniform Regular Reflection, Upper Branch of J

Figures 4.2 and 4.3, which are drawn for a value of a larger than a^*: the first sketch is on the boundary between subregions 2 and 4 in Figure 4.1, the second divides subregions 6 and 8.

It is plausible that for points (a, b) near (4.4) or (4.5) there will be a solution close to the respective uniform solutions. In fact, however, we can define two perturbation problems at each point in $\mathcal{R}$, one based on each of the two Riemann solutions at Ξ_A. In both cases, the solution will be piecewise constant outside an elliptic region, in which the solution will satisfy a degenerate elliptic free-boundary problem. The exact nature of the problem varies depending on which Riemann solution is selected and which of the eight subregions we are in. We conjecture that only for some of these problems will solutions exist; thus, there may be two, one or even no regular reflection type solutions for (a, b) in $\mathcal{R}$. Figure 4.4 describes the setup of the problem in one typical case (subregion 4).

In each case, the solution takes the following form: the shock S_2 is straight until it reaches the point Ξ_0, an admissible primary interaction. Then it continues as a curved shock. It eventually joins the point Ξ_A, which is therefore admissible in each case. What happens near Ξ_A depends on whether we are perturbing a Riemann solution which is subsonic at Ξ_A (the solution U_F in all cases and the solution U_R for values of a between $\sqrt{2}$

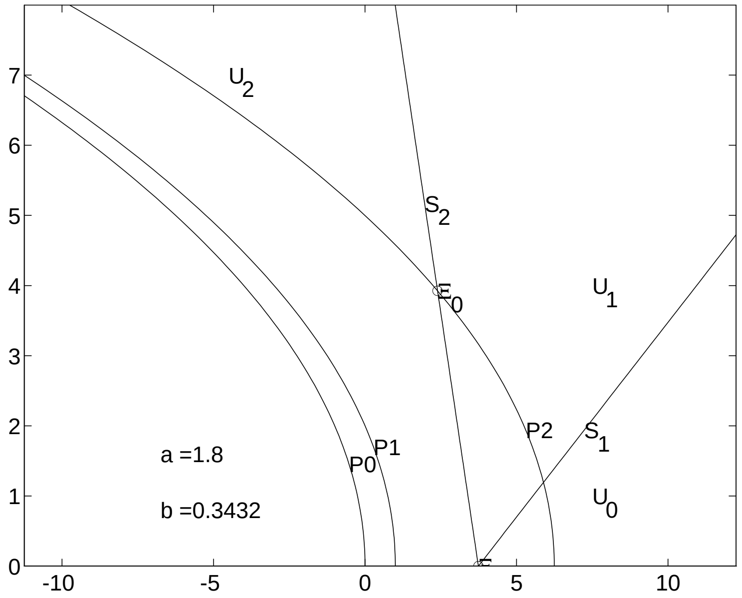

Figure 4.3: Uniform Regular Reflection, Lower Branch of J

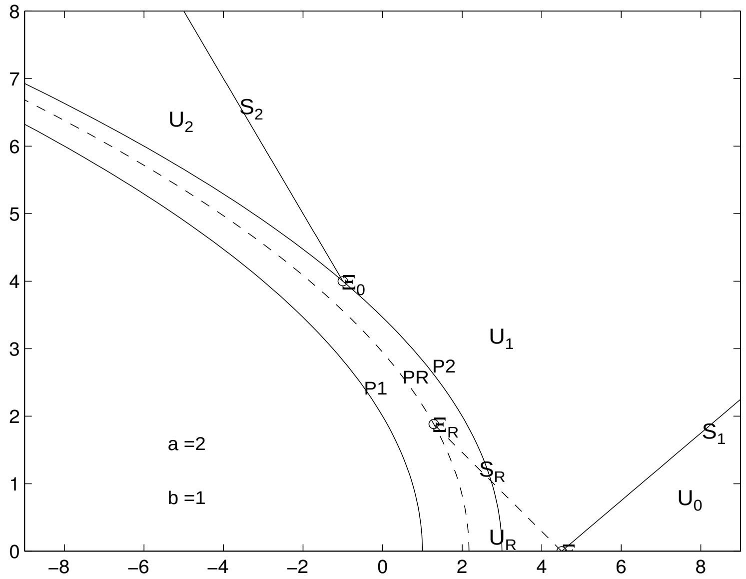

Figure 4.4: The Form of the Perturbed Reflection Problem in One Region (Subregion 4)

and a^*) or supersonic (the solution U_R when $a > a^*$). Figure 4.4 shows the second possibility: the Riemann problem at Ξ_A has a solution with middle state U_R and reflected shock S_R. The pair (U_R, Ξ_A) is hyperbolic, and thus the solution U is constant in a wedge outside the parabola P_R corresponding to U_R. A calculation shows that S_R intersects P_R at Ξ_R, where

$$\eta_R = \frac{2}{a - \sqrt{a^2 - 2}} \left(1 - \sqrt{a^2(2a^2 - 3) - a(2a^2 - 1)\sqrt{a^2 - 2}}\right)$$

and $\xi_R = \kappa_R \eta_R + \xi_A$. Between Ξ_0 and Ξ_R the shock is curved: it satisfies a free-boundary problem (based on the Rankine-Hugoniot equation) with the constant state U_1 upstream and an elliptic solution to (1.1) downstream. The elliptic problem has two degenerate boundaries: $U = U_2$ along P_2 between Ξ_0 and $-\infty$, and $U = U_R$ along P_R between Ξ_R and $\eta = 0$. The ξ-axis is an axis of symmetry of the problem, along which one has the boundary conditions $u_\eta = 0 = v$, and a boundary condition must be applied at the infinite boundary. The only other comment about this problem is that the relative position of the two parts of the degenerate boundary may affect the type of solution (singular [6] or regular [8]) to be expected: the two possibilities are $u_2 > u_R$ (subregions 4, 6, and 8) or $u_2 < u_R$ (subregion 2).

Although this solution is based on perturbing the uniform regular reflection, the perturbation is by no means small unless (a, b) is close to (4.4), and for $a > a^*$, and even then the solution may have a square root singularity at a point on the degenerate boundary as seen in [10].

If the Riemann solution at Ξ_A is subsonic, then the shock from Ξ_0 remains transonic all the way to Ξ_A. The elliptic problem now resembles the problem considered in [4] except that the bottom point, solution value and shock angle on the free boundary are now fixed.

4.2 The UTSD Prototype for von Neumann Reflection

There is another region of parameter space where we can reduce the problem to solving an elliptic equation. This is the case where $\Xi_1 \equiv S_1 \cap P_1$ is admissible. This requires the two conditions $\eta_1 > 0$ (so that Ξ_1 exists) and $a > I(b)$, so that Ξ_I is not admissible. The first condition, from Table 1, is $a < 1/\sqrt{2}$.

We describe the following reduction of the problem to a degenerate elliptic equation. Figure 4.5 pictures the important variables.

The solution has the constant value U_2 left of the shock S_2 up to the parabola P_2; the shock then becomes nonuniform, decaying and turning until it intersects S_1. At or before the point of intersection with S_1 it has

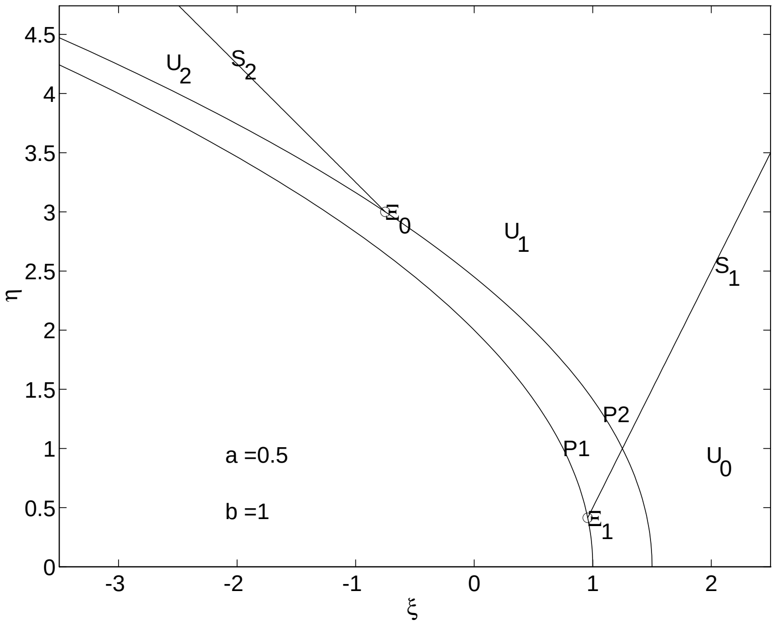

Figure 4.5: Hyperbolic Solution in von Neumann Reflection

zero strength. We expect this configuration to occur if S_1 intersects $\widetilde{S}_2$ after $\widetilde{S}_2$ becomes tangent to some sonic parabola P_T. Assuming small changes in the velocity u, and therefore even smaller changes in the position of the nonuniform shock, $\widetilde{S}_2$, (since the shock position is determined, via Rankine-Hugoniot conditions, as an integral of the velocity field), we replace $\widetilde{S}_2$ by S_2 to get an estimate for when this is the case. A simple calculation shows that the point of tangency, Ξ_T, is given by

$$\Xi_T = \left(1 + \frac{a}{2b} - b^2, 2b\right).$$

Therefore, we require that (a, b) lie above the curve M determined by the equation $\Xi_T = \Xi_I$:

$$a = M(b) \equiv \frac{1}{2b} - b. \tag{4.6}$$

This means, again supposing deviation from uniform flow is small, that the point $\widetilde{\Xi_I} = S_1 \cap \widetilde{S}_2$ lies on the right of Ξ_T.

Now, the shock S_1 is uniform until it reaches P_1; then it forms a free boundary between a nonuniform, subsonic solution and the upstream state U_0. As in the Mach stem case ([6], [7]), we expect the value of u at the foot of the shock to be larger than $u_1 = 1$; thus $u = 1$ is the minimum value of u

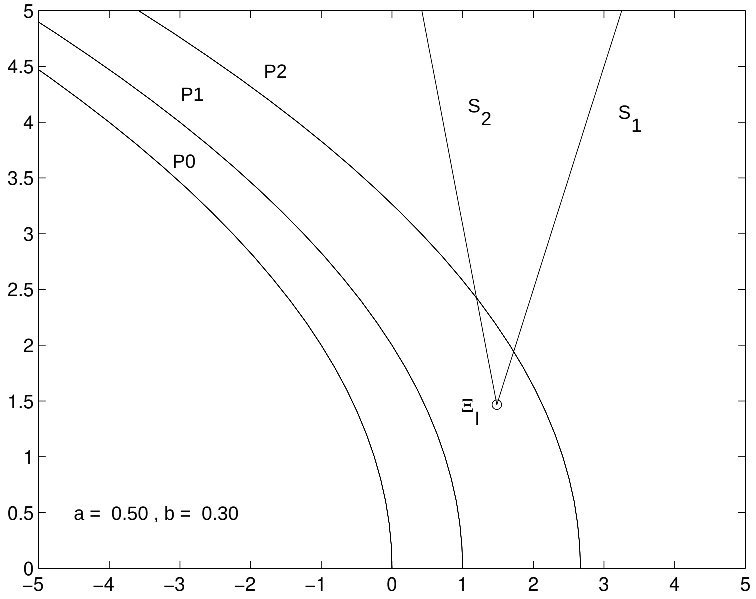

Figure 4.6: Geometry of Primary Curves in Transitional Mach Reflection

and is attained on the degenerate boundary, which we therefore expect to be singular. The elliptic problem in this case has two degenerate parts to its boundary – at P_2 and at P_1 – and two free-boundary problems arise. We expect that the solution at the degenerate boundary P_1 has a square-root type singularity at the point Ξ_1 where the shock S_1 intersects the sonic parabola P_1. Indeed, in [7] we showed that if the Mach stem $\xi = \xi(\eta)$ is an increasing, convex function, then the subsonic solution u is a decreasing function of η along the shock, and it must have a square-root singularity at the point where the Mach stem intersects the sonic curve. Numerical experiments in [10] confirm this scenario.

4.3 Transitional Mach Reflection

In the neighborhood of the region in (a, b)-parameter space in which Mach reflection takes place (Case 1), we expect to see a transition from Mach reflection to other types of reflection. In this spirit we pose the corresponding free-boundary problem and conjecture its solution in the region of parameter space bounded from below by the curve I and from above by M, defined by (4.6). We shall denote this region by $\mathcal{TMR}$. In Figure 4.6 we show the corresponding uniform shock configurations, related sonic curves and the important variables.

As in von Neumann reflection, the solution in this case has the constant value U_2 left of the shock S_2 up to the sonic parabola P_2. Then S_2 becomes nonuniform; we again call it $\widetilde{S}_2$. We assume that, as in von Neumann reflection, the shock strength of $\widetilde{S}_2$ is decaying, that is, the subsonic solution u, left of the shock $\widetilde{S}_2$, is decreasing as we move away from P_2. We shall assume that at the point, $\widetilde{\Xi_I}$, where $\widetilde{S}_2$ meets S_1, the state on the left of $\widetilde{S}_2$ is sonic. This is the only scenario that leads to the existence of a solution for the parameter values belonging to the region $\mathcal{TMR}$. However, unlike the case of von Neumann reflection, the shock strength at $\widetilde{\Xi_I}$ is not zero. Rather, at the point $\widetilde{\Xi_I}$ where the shock waves S_1 and $\widetilde{S}_2$ intersect, a degenerate hyperbolic wave interaction occurs. This degenerate hyperbolic interaction is the same as the one occurring for parameter values on the curve I (see the Remark at the end of Section 3). The following general result shows that the configuration of shock polars corresponds to region 4, and therefore there is a unique admissible solution which consists of a $-$-rarefaction wave, a constant state, U_m, and a $+$-shock wave between U_m and U_0.

Proposition 4.4 *Let $a \geq 1/\sqrt{2}$ and suppose that $\widetilde{\Xi_I}$ is any point on S_1. Then there is a unique value U_D on $S^+(U_1, \widetilde{\Xi_I})$ which is sonic at $\widetilde{\Xi_I}$. (The first condition means that U_D belongs to the $+$-shock branch of the downstream locus of U_1 at $\widetilde{\Xi_I}$.) Furthermore, there is a unique solution of the quasi-one-dimensional Riemann problem at $\widetilde{\Xi_I}$ with data U_0 and U_D, consisting of a shock beween U_0 and an intermediate state U_m, and a rarefaction wave between U_m and U_D.*

Proof: Since $\widetilde{\Xi_I}$ is on S_1, we have

$$\widetilde{\xi}_I = a\widetilde{\eta}_I + \frac{1}{2} + a^2$$

and if U_D is sonic then

$$u_D = \frac{\widetilde{\eta}_I^{\,2}}{4} + \widetilde{\xi}_I.$$

We can use these two equations to write

$$\frac{\widetilde{\eta}_I}{2} = -a + \sqrt{u_D - \frac{1}{2}}. \tag{4.7}$$

We note that if $a \geq 1/\sqrt{2}$, then there is a one-to-one correspondence between values $u_D \geq 1/2 + a^2 \geq 1$ and points on S_1 with $\widetilde{\eta}_I \geq 0$. Now $U_D \in S^+(U_1, \widetilde{\Xi_I})$ implies

$$v_D + a = (u_D - 1)\left(\frac{\widetilde{\eta}_I}{2} - \sqrt{\frac{\widetilde{\eta}_I^{\,2}}{4} + \widetilde{\xi}_I - \frac{u_D + u_1}{2}}\right) \tag{4.8}$$

(from the shock polar equation, (3.5), with $U_1 = (1, -a)$). Using (4.7) here, we obtain an equation for v_D in terms of u_D:

$$v_D = u_D\frac{\widetilde{\eta}_I}{2} - \sqrt{u_D - \frac{1}{2}} - \frac{(u_D - 1)^{3/2}}{\sqrt{2}}.$$

Now, in order for the Riemann problem between U_0 and U_D to have a unique solution consisting of a $+$-shock and a $-$-rarefaction wave, U_D must lie in region 4 of the downstream locus of U_0. To verify that U_D is in region 4, we compute the v-coordinates of the two sonic points on the shock loop $S(U_0, \widetilde{\Xi_I})$ and show that they bracket v_D. Using (3.5) again with $U_0 = (0, 0)$, we get

$$v_{max,min} = u_D \left(\frac{\widetilde{\eta}_I}{2} \pm \sqrt{\frac{\widetilde{\eta}_I^{\,2}}{4} + \widetilde{\xi}_I - \frac{u_D}{2}} \right) = u_D \left(\frac{\widetilde{\eta}_I}{2} \pm \sqrt{\frac{u_D}{2}} \right).$$

We require $v_{min} \leq v_D \leq v_{max}$; taking into account the expressions for v_{max}, v_{min} and v_D, we see the second inequality is always satisfied, and the first is equivalent to $F(u_D) \leq 0$ where

$$F(u) \equiv \sqrt{u - \frac{1}{2}} + \frac{(u-1)^{3/2}}{\sqrt{2}} - \frac{u^{3/2}}{\sqrt{2}}.$$

Calculating the derivative of F one sees that $F'(u) < 0$ on $[1, \infty)$. Therefore, since $F(1) = 0$, F is negative for all $u_D > 1$. This completes the proof. ■

We summarize our candidate for a transitional Mach reflection in the following conjecture, illustrated in Figure 4.7.

Conjecture If $(a, b) \in \mathcal{TMR}$ there will be a solution that consists of an incident shock, a reflected wave that meets the incident shock at a point $\widetilde{\Xi_I}$ above the wall, a Mach stem and a rarefaction wave emanating from $\widetilde{\Xi_I}$. The incident shock is uniform up to $\widetilde{\Xi_I}$, the reflected wave is uniform up to Ξ_0, transonic and nonuniform from Ξ_0 to $\widetilde{\Xi_I}$, and sonic at $\widetilde{\Xi_I}$. The rarefaction wave and Mach stem have the same structure as in the degenerate Case 1 problem arising along the curve I in (a, b)-parameter space.

Therefore, there is a small hyperbolic region consisting of a state U_m and a rarefaction wave between U_D and U_m that penetrates the region of subsonic flow. This is also seen in numerical experiments in [10].

4.4 A Mechanism for Mach Reflection with a Kink

In this section we conjecture the structure of the solution in the the region of (a, b)-parameter space that lies above the curve M, right of the line

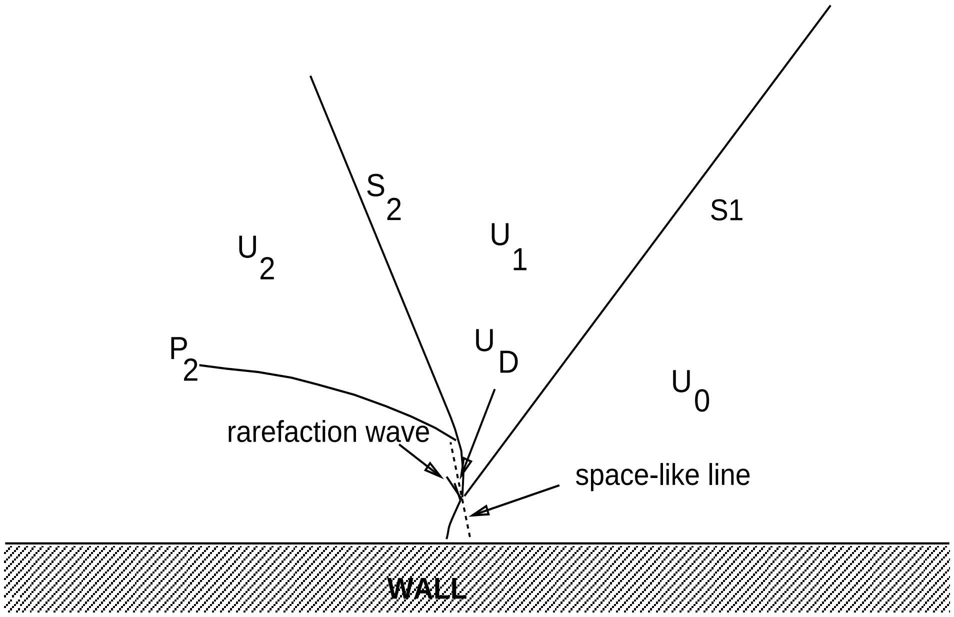

Figure 4.7: Transitional Mach Reflection

$a = 1/\sqrt{2}$, and left of the line $a = \sqrt{2}$. We call this region $\mathcal{KMR}$ because the structure of the solution we will describe in this section is a prototype of *kinky Mach reflection*.

The solution here is similar to the solution in region $\mathcal{TMR}$. Our solution consists of the constant state U_2 on the left of S_2 until S_2 reaches Ξ_0, the point of intersection with the parabola P_2. Then S_2 becomes nonuniform; call it again $\widetilde{S}_2$. The position of this transonic shock is determined by solving a free-boundary problem (the Rankine-Hugoniot conditions determine the position of the free boundary). The intersection of S_1 and $\widetilde{S}_2$ occurs at a point above the wall (since we are left of $a = \sqrt{2}$ in parameter space), with $\widetilde{S}_2$ having nonzero strength (because $a > 1/\sqrt{2}$). Again, let $\widetilde{\Xi_I} = (\widetilde{\xi_I}, \widetilde{\eta_I})$ denote the point of intersection between $\widetilde{S}_2$ and S_1, with $\widetilde{\eta_I} > 0$. We conjecture the following scenario for this interaction.

The shock $\widetilde{S}_2$, having traversed a subsonic region, is sonic again at the point, $\widetilde{\Xi_I}$, where it meets S_1, and is such that the resulting degenerate hyperbolic quasi-one-dimensional Riemann problem can be solved in the positive time-like direction. If this is the case, locally we have a degenerate hyperbolic quasi-one-dimensional Riemann problem of the same type as in the case of transitional Mach reflection. Again, by Proposition 4.4, at the point $\widetilde{\Xi_I}$ on S_1 there is a unique point U_D on the shock locus $S(U_1, \widetilde{\Xi_I})$ which is downstream from U_1 and is sonic at $\widetilde{\Xi_I}$. The degenerate Riemann problem at $\widetilde{\Xi_I}$ with data U_D and U_0 will again have a solution consisting of a shock and a rarefaction wave. The difference between this configuration and the prototype for transitional Mach reflection is that when $b >> 1$, the requirement that $\widetilde{S_2}$ approaches $\widetilde{\Xi_I}$ in the positive time-like direction in the neighborhood of $\widetilde{\Xi_I}$ implies that the shock $\widetilde{S_2}$ changes curvature from being concave up just beyond the point Ξ_0 where S_2 meets P_2 to being concave down near $\widetilde{\Xi_I}$, This is why we call this solution a kinky Mach reflection. If (a, b) is near the curve M, this configuration resembles transitional Mach reflection.

5. Conclusions

We now have a scenario for the wave interaction for every point in the (a, b)-parameter space, summarized in Figure 5.1. In the bifurcation diagram there are three curves that serve as sharp boundaries between different types of wave interactions. These are the curve I that serves as the boundary of Case 1, the region in the parameter space for which hyperbolic wave interactions take place (see Theorem 3.2); the line $a = \sqrt{2}$, on the left of which no symmetric shock reflection at the wall is possible (see Proposition 4.2); and the curve $a = J(b)$ along which uniform regular reflection takes place (see Proposition 4.3). Other regions may overlap and for those parameters the change between different types of wave interactions is smooth.

If we compare the proposed wave interactions, by region, with the theoretical and experimental predictions of Ben-Dor, [1] (see especially Figures 2.39, 2.41b, 2.45b and several of the later figures), we see there is a rough correspondence between the 'bifurcation diagram' in the $(M_s, \theta_{\rm w}^C)$ plane and the one that we are building in the (a, b) plane: the $(M_s, \theta_{\rm w}^C)$ diagram must be rotated 90 degrees counterclockwise and then reflected in a vertical axis for the correspondence to be apparent. The diagrams differ in some details like the persistence of the simple Mach reflection (SMR) region for large M_s (not necessarily supported by experiment) and the failure of SMR to occur at small M_s for large and small $\theta_{\rm w}^C$. However, as a qualitative picture of what this model may be capable of showing, namely the relation between different types of two-dimensional wave interactions as parameters vary, our picture shows some success: von Neumann reflection and regular reflection are far apart; in fact, they span the parameter space, and are separated by all the other modes of interaction. A significant difference is that there is a region devoted to 'double Mach reflection' in Ben-Dor's experimental and theoretical descriptions. Double Mach reflection may not occur in our simple model. We note, however, that the model was designed to describe transition between regular, von Neumann and simple Mach reflection at low

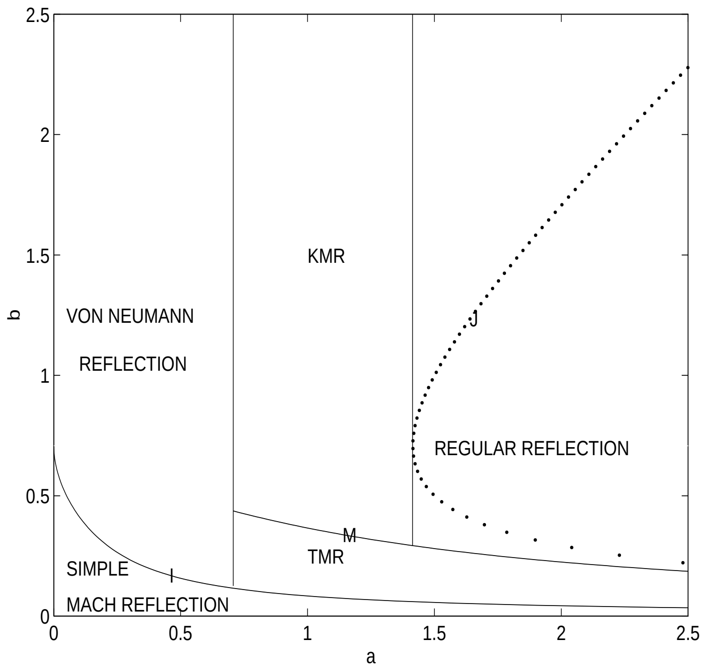

Figure 5.1: Wave Interaction Bifurcation Diagram

Mach numbers, where double Mach reflection does not occur, in theory. In our model, the strip $1/\sqrt{2} \le a \le \sqrt{2}$ contains transitional and kinky Mach reflection for large values of b and we conjecture that there is no further transition to double Mach reflection.

Our simplified model does not contain 'triple points' (see [3]). Of course, the full gas dynamics equations do not contain triple points either: a so-called triple point really consists of four states and four discontinuities, one being a slip line. However, our model does not permit slip lines. Here it may be noteworthy that no experimental results show a triple point with uniform states in all four quadrants: the flow behind the triple point is always nonuniform (though, on the scale of the problem, it may be close to constant). The simple Mach reflection which we described in Section 3.3 (Theorem 3) is the nearest this model comes to a triple point. Our candidate for Mach reflection is in fact a hyperbolic quasi-one-dimensional Riemann problem: there are four states rather than three and there is a small rarefaction wave as well as three shocks. This is exactly what the numerical simulations in [10] for Case 1 data indicate. (The calculations reported by Brio and Hunter, [3], do not include any Case 1 points.)

We have not yet completed the task of proving existence of the conjectured solutions to the free-boundary problems we have posed here. However, we have some evidence, from the solutions we have found to their fixed-boundary counterparts, that solutions do exist. The progress we have made in classifying different types of interaction patterns and the transitions between them supports our theme that shock interaction phenomena cannot be understood without examination of the full solution of the equations, particularly in the subsonic region. We believe that the paradoxes and their resolutions which appear in this simplified model have their counterparts, *mutatis mutandis*, in the full equations of gas dynamics.

References

[1] G. Ben-Dor. *Shock Wave Reflection Phenomena*. Springer-Verlag, New York, 1992.

[2] B. Boston. Front tracking of complex wave interactions. *Ph.D. Thesis*, SUNYSB-AMS-95-12, 1995.

[3] M. Brio and J. K. Hunter. Mach reflection for the two dimensional Burgers equation. *Physica D*, 60:194–207, 1992.

[4] S. Čanić and B. L. Keyfitz. A free-boundary problem for the two-dimensional unsteady transonic small disturbance equation. In preparation.

[5] S. Čanić and B. L. Keyfitz. Quasi-one-dimensional Riemann problems and their role in self-similar two-dimensional problems. UH Mathematics Department Research Report UH-MD-218, 1996, submitted.

[6] S. Čanić and B. L. Keyfitz. An elliptic problem arising from the unsteady transonic small disturbance equation. *Journal of Differential Equations*, 125:548–574, 1996.

[7] S. Čanić and B. L. Keyfitz. Oblique shock interactions and the von Neumann paradox. In B. Sturtevant, J. E. Schepherd, and H. G. Hornung, editors, *Shock Waves, Vol. I*, pages 435–440, Singapore, 1996. World Scientific.

[8] S. Čanić and B. L. Keyfitz. A smooth solution for a Keldysh type equation. *Communications in Partial Differential Equations*, 21:319–340, 1996.

[9] S. Čanić, B. L. Keyfitz, and D. H. Wagner. A bifurcation diagram for oblique shock interactions in the unsteady transonic small disturbance

equation. In J. Glimm et al., editors, *Proceedings of the Fifth International Conference on Hyperbolic Problems: Theory, Numerics, and Applications*, pages 178–187. World Scientific, Singapore, 1996.

[10] S. Čanić and D. Mirković. A numerical study of shock reflection modeled by the unsteady transonic small disturbance equation. submitted.

[11] P. Colella and L. Henderson. The von Neumann paradox for the diffraction of weak shock waves. *Journal of Fluid Mechanics*, 213:71–94, 1990.

[12] H. M. Glaz. Self-similar shock reflection in two space dimensions. In J. Glimm and A. Majda, editors, *Multidimensional Hyperbolic Problems and Computations*, volume IMA, 29, pages 89–106. Springer, New York, 1991.

[13] H. M. Glaz, P. Colella, I. I. Glass, and R. L. Deschambault. A numerical study of oblique shock-wave reflections with experimental comparisons. *Proceedings of the Royal Society of London*, A398:117–140, 1985.

[14] L. F. Henderson. Regions and boundaries for diffracting shock wave systems. *Zeitschrift für Angewandte Mathematik und Mechanik*, 67:73–86, 1987.

[15] A. Sakurai, L. Henderson, K. Takayama, Z. Walenta, and P. Colella. On the von Neumann paradox of weak Mach reflection. *Fluid Dynamics Research*, 4:333–346, 1989.

[16] R. J. Virgona. A study of shock wave diffraction from regular to irregular reflection and the effects of gas viscoisty. *Ph. D. Thesis, University of Sydney*, 1993.